THE ROLE AND APPLICATION OF QUANTUM CAPACITANCE IN NANOSTRUCTURED ENERGY STORAGE DEVICES

Hidenori Yamada[1], Prabhakar R. Bandaru[1,2]

[1]Department of Electrical and Computer Engineering, University of California, San Diego; 9500 Gilman Dr.; La Jolla, CA 92093, USA
[2]Department of Mechanical Engineering, University of California, San Diego; 9500 Gilman Dr.; La Jolla, CA 92093, USA

Keywords: carbon nanotubes, quantum capacitance, pseudocapacitance, electrochemical capacitors, energy storage

Abstract

Nanostructured electrochemical capacitors (ECs) are advantageous for charge and energy storage due to their intrinsically large surface area, which contributes to a large electrostatic/double layer capacitance (C_{dl}). However, the intrinsically small density of states in nanostructures results in a quantum capacitance (C_Q) in series with C_{dl} which could diminish the total device capacitance (C_{tot}). We investigate, through comparison with experiment, the relative magnitudes of C_{dl} and C_Q in electrodes constituted of carbon nanotube arrays. We will also present an equivalent circuit of C_{dl} and C_Q in series based on the voltage drop across C_Q. Consequently, we attribute the increase in C_{tot} resulting from ionizing radiation to an increased C_Q and suggest limits to the capacitance in ECs. A relation to pseudocapacitance will also be discussed.

Introduction

Electrochemical energy storage may be broadly classified as encompassing either batteries or electrochemical capacitors (ECs). While the former category incorporates devices with high energy density (~ 100 Wh/kg) and relatively low power density (~ 1 kW/kg), the latter comprises media with opposite attributes, *i.e.,* relatively lower energy density (~ 10 Wh/kg) and higher power density (~10 kW/kg)[1,2]. The overarching imperative is then to devise *intermediate* ECs, combining the best of both energy and power densities. Moreover, characteristics such as a high cycle life, *i.e.* the capability of rapid charging and discharging, for millions of cycles must be incorporated. Such ECs would therefore smoothly combine an electrical process (capacitor-like) and a chemical process (battery-like).

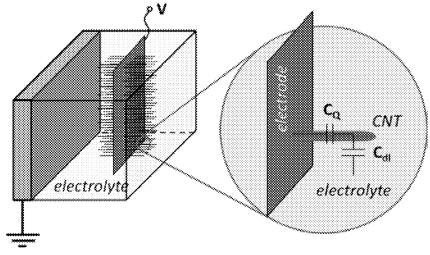

Figure 1 A schematic of electrode configuration in an electrochemical capacitor, zoomed into a section of the CNT array. C_Q and C_{dl} in series represented within a single CNT. As the surface area for the CNT electrode (in red) is much higher than that of the counter electrode (in green), the capacitance of the former is much more significant. [23]

Much EC work has focused on charge storage in a *double layer* comprised of the electrode charge and electrolyte charge of opposite polarity – Figure 1. The double layer capacitance/unit area (C_{dl}) is directly proportional to the dielectric constant ($\varepsilon=\varepsilon_o\varepsilon_r$, where ε_o is the permittivity of free space and is equal to $8.854\cdot10^{-12}$ F/m and ε_r is the relative permittivity, *e.g.,* ~ 80 for water) and inversely proportional to the charge separation distance between the positive (+) and negative (-) charges. C_{dl} is further constituted of a *Helmholtz* capacitance, where distances are of the order of the electrolyte ionic diameters, as well as a *diffusive* capacitance, with mean distances of the order of the Debye length[3] ($d=\sqrt{\frac{\varepsilon k_B T}{2N_A(ze)^2 I}}\sim 9.78\frac{1}{\sqrt{I}}$ nm) where k_B (=$1.38\cdot10^{-23}$ J/K) is the Boltzmann constant, T is the absolute temperature (K), N_A (= $6.02\cdot10^{23}$ atoms/mole) is the Avogadro number, (ze) is the net charge with e as the elementary electronic charge (=$1.6\cdot10^{-19}$ C), and I (in moles/m^3) is the electrolyte concentration. For an aqueous electrolyte (@ 1 M concentration), C_{dl} could then *potentially* be of the order of 250 μF/cm^2. The utilization of a high surface area electrode substrate, *e.g.,* carbon nanotubes (CNTs), where the total surface area would be much larger[4] than the projected area would also be beneficial. However, the values reported in literature are typically an order of magnitude lower[5], and this has been tentatively ascribed to incomplete/inadequate utilization of the surface area[6].

In previous studies[8,9], it was found that ion irradiation, facilitated through plasma processing, increased the observed C_{tot}. However, details of the underlying mechanisms were not specified. In this article, we propose a possible mechanism through detailed comparison with experiment and seek to understand the limits of capacitance that may be manifested with a given CNT configuration. The underlying principles may be adapted to other nanostructure and device types as well.

Also, a substantial addition to the total capacitance (C_{tot}) through the utilization of *parallel* redox capacitance/pseudocapacitance (C_p), which mimics battery like behavior[7], could also be obtained in ECs as discussed in a previous study[8,9]. The Randles-Sevcik equation is usually cited to explain C_p, starting from the assumption that ion transport is caused by diffusion. We propose an alternative derivation, assuming that ion transport is instead caused by electrical drift.

Quantum Capacitance

We considered quantum capacitance (C_Q), which is relevant when nanostructures such as CNTs, with a finite density of states (DoS) $D(E)$. The increase (/decrease) of the Fermi energy (E_F) of the CNTs could be significant, relative to the bulk electrolyte, when charge carriers of a single type, *e.g.,* electrons of magnitude dQ (= $e\cdot dn$), are added (/removed) due to an applied voltage change (dV)[10]. An effective capacitance could therefore be defined for a given electrode, considering the DoS at the E_F, as follows:

$$C_Q=\frac{dQ}{dV}=\frac{edn}{\frac{1}{e}dE_F}=e^2D(E_F) \tag{1}$$

We model the *net* device capacitance in Figure 1 as a series combination of C_{dl} *and* C_Q. If, as hypothesized[8,11], the role of ion irradiation (*e.g.,* through plasma processing) was to introduce

fixed charges, then C_Q increases significantly with increasing processing time. The series combination of C_Q and C_{dl} would allow an increase in C_{tot} consistent with the experiment as can be understood through:

$$\frac{1}{C_{tot}} = \frac{1}{C_{dl}} + \frac{1}{C_Q} \tag{2}$$

It should be pointed out that our work focuses on correlating the capacitance contributions from MWNTs (with concentric nanotubes of gradually decreasing perimeters) while previous works, *e.g.,* by Fang, *et al*[12] and Xia, *et al*[13], are on graphene sheets or nanoribbons, the latter of which have sub-bands due to the finite width and become graphene sheets in the infinite width limit. The C_Q of for nanoribbons and graphene was discussed in Ref. 12 for MOSFET (metal oxide semiconductor field effect transistor)-like devices. While they discussed the series addition of the gate oxide capacitance and the C_Q, we discuss the series addition of the double layer capacitance (C_{dl}) with the C_Q as appropriate for an electrochemical capacitor. The maximum carrier concentration (n) studied in Ref. 12 was less than $2\cdot10^{12}$/cm^2 with concomitant C_Q values of the order of 10 μF/cm^2, which seem to be comparable with the values calculated in this article. In Ref. 13, they fabricated experimental MOSFET-like devices using a graphene sheet and analyzed their data. Accordingly, there was no need to consider sub-band contributions, but for our purposes, counting contributions of several tens of all relevant sub-bands is critical and that is what will be performed below.

We modeled multi-walled CNT (MWCNT) characteristics, in accordance with previous experiments which used such ensembles (with average individual MWCNT diameter of 20 nm and spacing 200 nm on a 5 mm × 5 mm Si substrates) as electrodes[8,11]. We calculated the DoS of a constituent wall in a MWCNT, following previous methodology[10,14], modeled as a rolled graphene sheet (infinite in the y-direction and both periodic and finite in the orthogonal x-direction). It was assumed that the walls are independent of each other[15], with the implication that the total DoS can be obtained as the sum of the DoS for each constituent wall. We considered zigzag CNTs (involving rolling of the graphene sheet in the x- direction), as this category encompasses both semiconducting and metallic CNTs[16]. As we consider relatively large diameter CNTs[11], the details as to how graphene is rolled to yield CNTs, *i.e.,* whether zigzag or armchair or chiral[17], will not influence the C_Q. The exact dispersion relation for a graphene sheet, through the tight-binding approximation[10,18] is:

$$E(k_x, k_y) = \pm\gamma_1\sqrt{1 + 4\cos\left(\frac{\sqrt{3}ak_y}{2}\right)\cos\left(\frac{ak_x}{2}\right) + 4\cos^2\left(\frac{ak_x}{2}\right)}\,. \tag{3}$$

In (3), $a = \sqrt{3}\,a_0$ where a_0 (= 0.142 nm) is the C- C bond length and the overlap integral γ_1 = 2.9 eV[15]. The 20 nm MWCNT with 15 walls was *approximately* indexed through [N, *0*] (with N = 250 for the outermost wall, and decreasing by 10 for each successive inner wall), and was effectively one dimensional since $k_{x,n} = \frac{2q\pi}{Na}$ (q: sub-band index), while k_y is continuous. The DoS for a single sub-band is then $\frac{4}{2\pi}\frac{dk_y}{dE}$ with k_{xn} held constant, and the 4 in the numerator accounted for the electron spin degeneracy and the positive/negative k_y.

Since C_Q is a function of E_F from (1), we needed to estimate an appropriate value for E_F. In a graphene sheet with no impurities, each carbon atom provides one electron to the p_z orbital, yielding semi-metallic behavior and implying[19] an E_F = 0 eV, and zero carrier density (n) at T = 0 K. However, n could range around 4.6 · 10^{12} cm^{-2}, corresponding to the two-dimensional carrier density interpolated from the experimental value for bulk graphite[15] of 10^{19} cm^{-3}, i.e., through $(10^{19})^{2/3}$. With variability in n, e.g., due to defects[13], etc., attempting an exact E_F would yield imprecise values, and it could then be appropriate to estimate n by approximating the CNTs as sheets of graphene and calculating the DoS, as was done here. The n of 4.6·10^{12}/cm^2 is then only posited as a representative number for the purpose of illustrating the concepts. The actual n in any sample could either be below or above[20] this number with a corresponding decrease/increase in the C_Q.

From the total carrier concentration at the Fermi energy, $n(E_F) = \int_0^\infty D(E) f(E) dE$. The $f(E)$ is the Fermi-Dirac function and was approximated as a step function in our calculations, as the difference between the value of $f(E)$ with a finite temperature (T=300 K) and with T = 0 K was at most 5 %. The E_F values were found to range around 278 meV (with n = 4.6 · 10^{12} cm^{-2}). Computing $E_F(k_{x,n}, k_y)$ from (3), and then $C_Q(k_{x,n}, k_y)$ from (1), pairs of E_F and C_Q for all sub-bands $k_{x,n}$ over the Brillouin zone for k_y are plotted. $C_Q(E_F)$ is constant initially due to the metallic CNTs, up to ~ E_F = 50 meV, due to the constituent metallic NTs with finite and constant DoS, where C_Q does not increase as there is no sub-band contribution from the NTs. The staircase like structure in the variation results from the contribution of successive sub-bands to the DoS. At E_F = 278 meV we estimate, in units of capacitance per NT length, C_Q = 48 fF/μm. The linearity in the plot justifies starting with the graphene E_F-k relation to estimate the E_F of the CNT from n.

Incorporating Double-Layer Capacitance

We next consider the two major components, which add in series, of the C_{dl}: (i) a *Helmholtz* capacitance (C_H) due to a Coulombic attraction, and (ii) a *Gouy-Chapman* (C_{GC}) capacitance due to the diffusive distribution of ions in the electrolyte[3]. An area average C_H can be computed from a spatial separation corresponding to the ionic radius[11] (*e.g.,* r ~ 0.278 nm for K^+ ions in $K_3Fe(CN)_6$) and is equal to ε/r. The C_{GC} is estimated from the voltage drop (ϕ) across the diffusive region (which is of the order of the Debye length, d) and is equal to (ε/d) $cosh$ ($e\phi/2k_BT$). Consequently,

$$\frac{1}{C_{dl}} = \frac{r}{\varepsilon} + \frac{d}{\varepsilon}\frac{1}{\cosh\left(\frac{e\phi}{2k_BT}\right)} \qquad (4)$$

At smaller ϕ ($\rightarrow$ 0) the $C_{dl} \rightarrow C_{GC}$, at ϕ (~ $3k_BT$) the C_H and C_G are comparable, and at a larger ϕ (> $10k_BT$), the $C_{dl} \rightarrow C_H$. With a range of ϕ from zero to 278 mV (corresponding to the E_F), we estimate from (4), a range of C_{dl} for an electrolyte concentration, I (in moles/m^3), from ~ $7.3\sqrt{I}$ μF/cm^2 to ~ 255 μF/cm^2. In order to compare to the one-dimensional quantum capacitance C_Q estimated above, we convert the units of C_{dl} by multiplying by $2\pi r$, where r = 10 nm is the outer MWCNT wall radius. The corresponding range is then from $4.6\sqrt{I}$ fF/μm to 160 fF/μm. For a given I, say 3 mM as in the experiments (see Table V of Ref. 11), the C_{dl} is calculated to be 7.9 fF/μm. With C_Q = 48 fF/μm, this results in a C_{tot} ~6.8 fF/μm. Generally, the

electrostatic interaction between surfaces of different geometries decays with a characteristic decay length equal to the Debye length[21]. Equivalent capacitances are then obtained for the planar/cylindrical cases.

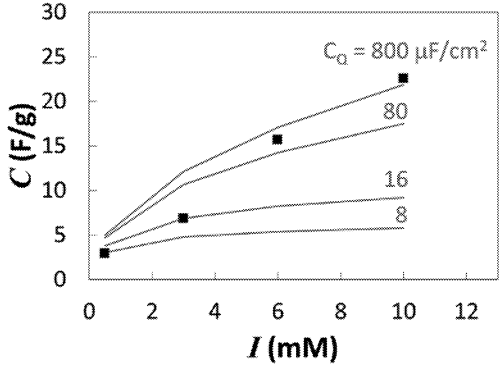

Figure 2 Comparison of experimentally measured capacitance (see Ref. 11) in ■ with numerical estimates (red lines) of C_Q, as a function of electrolyte concentration, I. A value of C_Q = 80 μF/cm^2 corresponds to the theoretically predicted C_Q = 48 fF/μm. The match is strongest for low I with low C_Q and for high I with high C_Q. [23]

The capacitance per projected electrode area is the product of the obtained C_{tot}, the average CNT length, L (= 100 μm), the estimated CNT density on the substrate, λ (~ $2.5 \cdot 10^9$ cm^{-2}), and the projected surface area of the electrode, A (~ 0.25 cm^2) yielding an expected capacitance value per projected area of ~ 1700 μF/cm^2. Dividing this value by the weight of the CNTs (~ 40 μg), the capacitance values, in F/g, were computed and are shown in comparison to the experimental values (details have been previously reported[8,11]) in Figure 2. The figure then indicates the relative magnitudes of C_Q relevant to the measured capacitances and indicates a variable C_Q, being more significant (for a series combination of C_{dl} and C_Q) at lower electrolyte concentrations when the CNT is sufficiently isolated so that its DoS is small. We generally observe from the figure that while higher electrolyte concentrations may be adequately modeled through the use of C_{dl} alone, lower concentrations need C_Q as well. C_Q is significant when the CNT is sufficiently isolated so that its DoS is small. As I increases, charge transfer between CNT and electrolyte may be more likely, reducing isolation and increasing the CNT DoS effectively so that C_Q increases and becomes insignificant, as per equation (2).

Pseudocapacitance: Drift vs. Diffusion

Finally we consider the source of C_p, which is attributed to a redox reaction occurring between the EC plate and the electrolyte ions[7]. When calculating the peak current according to the Randles-Sevcik derivation, the limiting mechanism is considered to be ion diffusion and is therefore based on the diffusion equation.

$$\frac{M_O(x=0,t)}{M_R(x=0,t)} = \exp\left(\frac{NF}{RT}\left(E_i - vt - E^{0'}\right)\right) \tag{5}$$

$$\frac{\partial M_O(x,t)}{\partial t} = D_O \frac{\partial^2 M_O(x,t)}{\partial x^2}; \quad M_O(x,0) = M_O^*, \quad M_O(\infty,t) = M_O^*$$
$$\frac{\partial M_R(x,t)}{\partial t} = D_R \frac{\partial^2 M_R(x,t)}{\partial x^2}; \quad M_R(x,0) = 0, \quad M_R(\infty,t) = 0 \tag{6}$$

$$D_O\left(\frac{\partial M_O(x,t)}{\partial x}\right)_{x=0} + D_R\left(\frac{\partial M_R(x,t)}{\partial x}\right)_{x=0} = 0 \tag{7}$$

where M_O and M_R are the molar concentrations for the oxidized ions and reduced ions, respectively[24], x is distance from the electrode plate, N is the number of electrons per reaction, F is the Faraday constant, R is the ideal gas constant, E_i is the initial potential at which no reaction occurs, $E^{0'}$ is the energy corresponding to the Fermi level, and D_O and D_R are the diffusion constants for the oxidized ions and reduced ions, respectively. The ensuing derivation involves convolution of the Laplace transform of the diffusion equation, assuming uniform distribution at $t = 0$ and stationary concentration infinitely far away from the plate.

$$I = 0.4463 N^{3/2} e n_{elec} A \sqrt{\mu \nu} \tag{8}$$

Here, e is the elementary charge, n_{elec} is the electrolyte ion concentration in cm^{-3}, A is the electrode total area, μ is the electrolyte ion mobility (related to the ion diffusion constant), and ν is the sweep rate.

We postulate here a derivation based on drift rather than on diffusion based on the idea that at higher sweep rates, more electric field leaks through the double-layer as shown in Fig. 3. The ions move in response to the field, which points to electrical drift as the ion transport mechanism, rather than in response to concentration gradient.

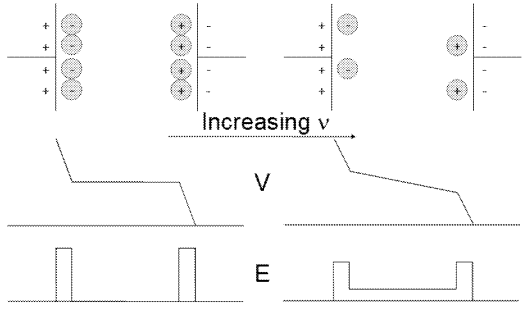

Figure 3 Schematic voltage and electric field profiles across an ultracapacitor (CNTs not shown here). With increasing sweep rate ν, the double layer does not form as smoothly, allowing electric field to leak into the bulk electrolyte and apply force to the electrolyte ions. This process is assumed to be drift rather than diffusion.

The starting equation is therefore $v = \mu E$ where v is ion velocity, μ is ion mobility, and E is electric field. We can relate E and ν by performing

$$E = \frac{dV}{dx} = \frac{dV/dt}{dx/dt} = \frac{\nu}{v}, \tag{9}$$

resulting in the form $v^2 = \mu\nu$. Finally, since $I = JA = en_{elec}vA$, we have

$$I = en_{elec}A\sqrt{\mu\nu}. \tag{10}$$

This differs from the known Randles-Sevcik equation by $N^{3/2}$ (which is 1 for most electrolyte redox reactions) and by the constant factor 0.4463, preserving the well-established factors of n and $\nu^{1/2}$.

Conclusion

Several insights are obtained through our analyses. For example, the magnitudes of both C_Q and C_{dl} are comparable and suggest an explanation for the considerable (up to 300 %) increase in C_{tot} when the CNT constituted electrodes are subject to argon plasma processing[8,11]. Such exposure was hypothesized to introduce charged acceptor like defects into the CNT's carbon lattice, through argon abstracting electronic charge from the carbon bonds. Much like surface states in semiconductors[22], the fixed charges in the CNT lattice are immobile, and do not respond to applied voltage and would not contribute directly to the C_{dl}. However, the added charge density (which would be proportional to the exposure time) affects the Fermi energy and enhances C_Q. A higher C_Q closer to C_{dl} enhances the maximum C_{tot} that could be obtained from a given system. We can also conclude that the limits to the magnitude of the capacitance that can be obtained from CNT or nanostructure based electrochemical capacitors is a function of the series combination of *both* the electrostatic/double layer capacitance as well as the quantum capacitance. In a situation where both are comparable, one would need to increase the C_Q, say through varying the charge density and maximize the total capacitance.

Assuming drift over diffusion as the main mechanism for ion transport within the electrolyte allows for an analytical derivation of the CV current peak, resulting in an expression with the same functional form as the Randles-Sevcik equation, differing only by a constant factor of 0.4463. Drift, which is dependent on spatial voltage gradient, is faithful to the CV experiment because it relates current output to voltage input. More precisely, the known sweep rate (temporal voltage gradient) can be related to the necessary spatial voltage gradient if we know ion velocity, which is related to the known diffusion rate by the Einstein relation.

Acknowledgments

This work was supported by the US National Science Foundation under grant ECS-0643761. The authors thank Professor P. M. Asbeck for useful discussions, as well as Dr. M. Hoefer and Professors P. Yu and Y. Taur for relevant comments.

References

1 J. R. Miller and A. F. Burke, The Electrochemical Society Interface**, 17,** 53-57 (2008).

2 J. M. Miller, *Ultracapacitor Applications* (The Institution of Engineering and Technology, Herts, UK, 2011).

[3] A. J. Bard and L. R. Faulkner, *Electrochemical Methods: Fundamentals and Applications*, 2 ed. (John Wiley, New York, 2001).
[4] A. Peigney, C. Laurent, E. Flahaut, R. R. Basca, and A. Rousset, Carbon **39,** 507-514 (2001).
[5] P. Simon and Y. Gogotsi, Nature Materials **7,** 845-854 (2008).
[6] L. R. Radovic, in *Carbons for electrochemical energy storage and conversion systems*, edited by F. Beguin and E. Frackowiak (CRC Press, New York, 2010).
[7] B. E. Conway, Journal of the Electrochemical Society **138,** 1539-1548 (1991).
[8] M. Hoefer and P. R. Bandaru, Applied Physics Letters **95,** 183108 (2009).
[9] J. A. Nichols, H. Saito, M. Hoefer, and P. R. Bandaru, Electrochemical and Solid State Letters **11,** K35-K39 (2008).
[10] S. Datta, *Quantum Transport: Atom to Transistor* (Cambridge University Press, New York, 2005).
[11] M. Hoefer and P. R. Bandaru, Journal of Applied Physics **108,** 034308 (2010).
[12] T. Fang, A. Konar, H. Xing, and D. Jena, Applied Physics Letters **91,** 092109 (2007).
[13] J. Xia, F. Chen, J. Li, and N. Tao, Nature Nanotechnology **4,** 505-509 (2009).
[14] L. Forro and C. Schonenberger, in *Carbon Nanotubes- Topics in Applied Physics*; *Vol. 80*, edited by M. S. Dresselhaus, G. Dresselhaus, and P. Avouris (Springer-Verlag, Heidelberg, 2001).
[15] R. Saito, G. Dresselhaus, and M. S. Dresselhaus, Physical Review B **61,** 2981-2990 (2000).
[16] P. R. Bandaru, Journal of Nanoscience and Nanotechnology **7,** 1239-1267 (2007).
[17] R. Saito, M. Fujita, G. Dresselhaus, and M. S. Dresselhaus, Applied Physics Letters **60,** 2204-2206 (1992).
[18] C. Beenakker, Reviews of Modern Physics **80,** 1337-1354 (2008).
[19] M. I. Kastnelson, *Graphene: Carbon in Two Dimensions* (Cambridge University press, Cambridge, UK, 2012).
[20] D. K. Efetov and P. Kim, Physical Review Letters **105,** 256805 (2010).
[21] J. N. Israelachvili, *Intermolecular and Surface Forces,*, 3 ed. (Academic Press, San Diego, 2011).
[22] J. Bardeen, Physical Review **71,** 717-727 (1947).
[23] H. Yamada and P. R. Bandaru, Applied Physics Letters **102,** 173113 (2013).
[24] The original text uses C_O and C_R: please do not confuse these for capacitances. These are molar concentrations.